U. S. Department of Commerce
National Bureau of Standards

Research Paper RP1880
Volume 40, May 1948

Part of the Journal of Research of the National Bureau of Standards

# Perforated Cover Plates for Steel Columns: Summary of Compressive Properties

By Ambrose H. Stang and Martin Greenspan

Eighty-eight steel perforated cover plate columns have been tested in the elastic range. The experimental axial rigidity under compressive load of the uniformally perforated lengths has been compared with theoretical values. The agreement in general was very good.

The distribution of stress on the edge of the perforation of these columns was also measured. The maximum values of stress concentration found experimentally have been compared with theoretical values obtained for a single hole in a large plate. These experimental values also in general agreed with the theoretical values.

The values of the average stress on the net area for the compressive tests to destruction of 28 perforated plate columns were in nearly all cases greater than the maximum stress at failure for columns of the same size having solid plates.

## I. Introduction

This paper summarizes the results of compressive tests of steel colums having perforated cover plates. Tests have been made of perforated plate columns with perforations of the following shapes: Circular, ovaloid with the load parallel to the long axis, ovaloid with the load parallel to the short axis, elliptical with the load parallel to the major axis, "square" with the load parallel to two sides, and "square" with the load parallel to a diagonal.

In this paper, the ovaloid perforations were those having the shape of a square with a semicircle erected on two opposite sides; the "square" perforations were squares with rounded corners, the radius of the fillets being about 0.086 times the length of the side of the square. The expression "perforated plate" is used here for a plate having a series of similar perforations uniformly distributed along its length.

Tests in the elastic range have been made on 88 columns with perforated plates and on 17 columns with solid plates. Maximum compressive-load tests have been made on 28 columns with perforated plates and on 4 with solid plates.

The Research Paper [1] [1] containing the original program outlined the need for the tests and described the columns and the testing procedure. The results of these tests are given in four Research Papers [2]. The results of additional tests are given in two other Research Papers [3, 4]. The details of the columns have been given in those Research Papers. The essential data describing them are given in table 1.

Two papers dealing with the theoretical axial rigidity of perforated cover plate columns have been written by Martin Greenspan [5, 6]. He has also written a paper [7] on the theoretical stress distribution in a plate with a small hole. In the present paper the results of the tests in the elastic range will be compared with the theoretical values, and the results of the maximum-load tests will be discussed.

[1] Figures in brackets indicate the literature references at the end of this paper.

TABLE 1. *Description of columns*

[Nominal dimensions: Plate thickness, ⅜ in. Perforations equally spaced about midheight of column]

| Column designations | Number of angles | Perforation | | | | Load parallel to— | Plate width, $w$ |
|---|---|---|---|---|---|---|---|
| | | Number | Shape | Breadth, $b$ | Spacing, $s$ | | |
| COLUMNS 14 FT. 9 IN. LONG; ANGLES 8 BY 4 BY ½ IN. | | | | | | | |
| | | | | *in.* | *in.* | | |
| C1A | 4 and 2 | 4 | Circle | 9.00 | 21.0 | Diameter | 20.0 |
| C1B | 4 and 2 | 4 | do | 9.00 | 33.0 | do | 20.0 |
| C1C | 4 and 2 | 4 | do | 9.00 | 45.0 | do | 20.0 |
| C2A | 4 and 2 | 3 | Ovaloid | 6.75 | 25.5 | Long axis | 15.0 |
| C2B | 4 and 2 | 3 | do | 6.75 | 37.5 | do | 15.0 |
| C2C | 4 and 2 | 3 | do | 6.75 | 49.5 | do | 15.0 |
| C3A | 4 and 2 | 3 | do | 9.00 | 30.0 | do | 20.0 |
| C3B | 4 and 2 | 3 | do | 9.00 | 42.0 | do | 20.0 |
| C3C | 4 and 2 | 3 | do | 9.00 | 54.0 | do | 20.0 |
| C4A | 4 and 2 | 3 | do | 11.50 | 35.0 | do | 25.5 |
| C4B | 4 and 2 | 3 | do | 11.50 | 47.0 | do | 25.5 |
| C4C | 4 and 2 | 3 | do | 11.50 | 59.0 | do | 25.5 |
| C4E | 2 | 3 | do | 6.50 | 37.0 | do | 25.5 |
| C4F | 2 | 3 | do | 16.50 | 57.0 | do | 25.5 |
| C4G | 2 | 3 | Ellipse | 11.50 | 47.0 | Major axis | 25.5 |
| C4H | 2 | 3 | Ovaloid | 11.50 | 29.75 | Short axis | 25.5 |
| C4I | 2 | 3 | Square | 11.50 | 35.5 | Side | 25.5 |
| C4J | 2 | 3 | do | 11.67 | 36.0 | Diagonal | 25.5 |
| COLUMNS 10 FT. 0 IN. LONG; ANGLES 6 BY 4 BY ½ IN. | | | | | | | |
| C6 | 4 | 3 | Circle | 10.00 | 30.0 | Diameter | 30.0 |
| C7 | 4 | 2 | Ovaloid | 10.00 | 44.0 | Long axis | 30.0 |

## II. Axial Rigidity

The axial rigidity is described by a factor, $K$, defined as the ratio of the axial rigidity of a column having a perforated plate to the axial rigidity of an unperforated, but otherwise similar, column. The axial rigidity factor $K$ is then defined so that $KEA_g$ is the rigidity that should be used in place of $EA_g$ in the ordinary formula for computation of the extension (or shortening) of the member. Here $E$ is the modulus and $A_g$ the gross area of the member.

For a column having angles and a perforated plate, the experimental axial rigidity factor is

$$K=\frac{E'_p}{E'_s} \tag{1}$$

where $E'_p$ is the effective modulus (based on gross area) for a perforated cover plate column, and $E'_s$ is the modulus for a solid plate column of the same gross cross-sectional area and of the same material.

The experimental axial rigidity factor $K$ for the perforated plate by itself may be calculated from the results of the column test, as shown on p. 680 of reference [1], by the formula

$$K=\frac{E'_p}{E'_s}\left(1+\frac{A_A}{A_P}\right)-\frac{A_A}{A_P} \tag{2}$$

where $A_A$ is the cross-sectional area of the angles and $A_P$ the gross cross-sectional area of the perforated plate.

The theoretical axial rigidity factor $K$ for a plate or column is given by the equation [5, 6]

$$\frac{1}{K}-1=\frac{f}{C(n)}\frac{V_o}{V_g} \tag{3}$$

where

$f$=a constant depending on the shape of the perforation and the direction of the applied load.

$$C(_n)=1-\frac{1}{2n^2} \tag{4}$$

$n=A_g/(A_g-A_n)$, $A_g$ being the gross and

$A_n$ the net cross-sectional area of the member (column or plate)

$V_o$=the volume of the perforation

$V_g$=the gross volume of one bay of the member.

Values of the constant $f$ of eq 3 for various cases are given in table 2.

TABLE 2. *Values of f in equations 3 and 5*

| Perforation | Load parallel to— | $f$ | |
|---|---|---|---|
| | | eq 3 | eq 5 |
| Circle | Diameter | 3.000 | 4.713 |
| Ellipse, semiaxes, $a$ and $b$ | Major axis, $a$ | $1+(2b/a)$ | $1.571\ \frac{1+2b/a}{b/a}$ |
| Do | Minor axis, $b$ | $1+(2a/b)$ | $1.571\ \frac{1+2a/b}{a/b}$ |
| Ovaloid | Long axis | 2.048 | 7.313 |
| Do | Short axis | 4.968 | 4.435 |
| Square | Side | 2.989 | 5.940 |
| Do | Diagonal | 3.596 | 3.962 |

The theoretical axial rigidity factor $K$ for a perforated plate of uniform thickness (by itself and

without angles) may be derived from eq 3 and put in the form.

$$\frac{1}{K}-1=f\frac{w}{s}\frac{(b/w)^2}{2-(b/w)^2}, \qquad (5)$$

where

$b$ = perforation width
$w$ = plate width
$s$ = perforation spacing.

Values of the constant $f$ of eq 5 for various cases are given in table 2.

Nomographic charts for the solution of eq 5 are shown in figure 1 for plates having ovaloid perforations, in figure 2 for plates having elliptical perforations and in figure 3 for plates having square perforations, for limited ranges of the ratios $b/w$ and $w/s$.

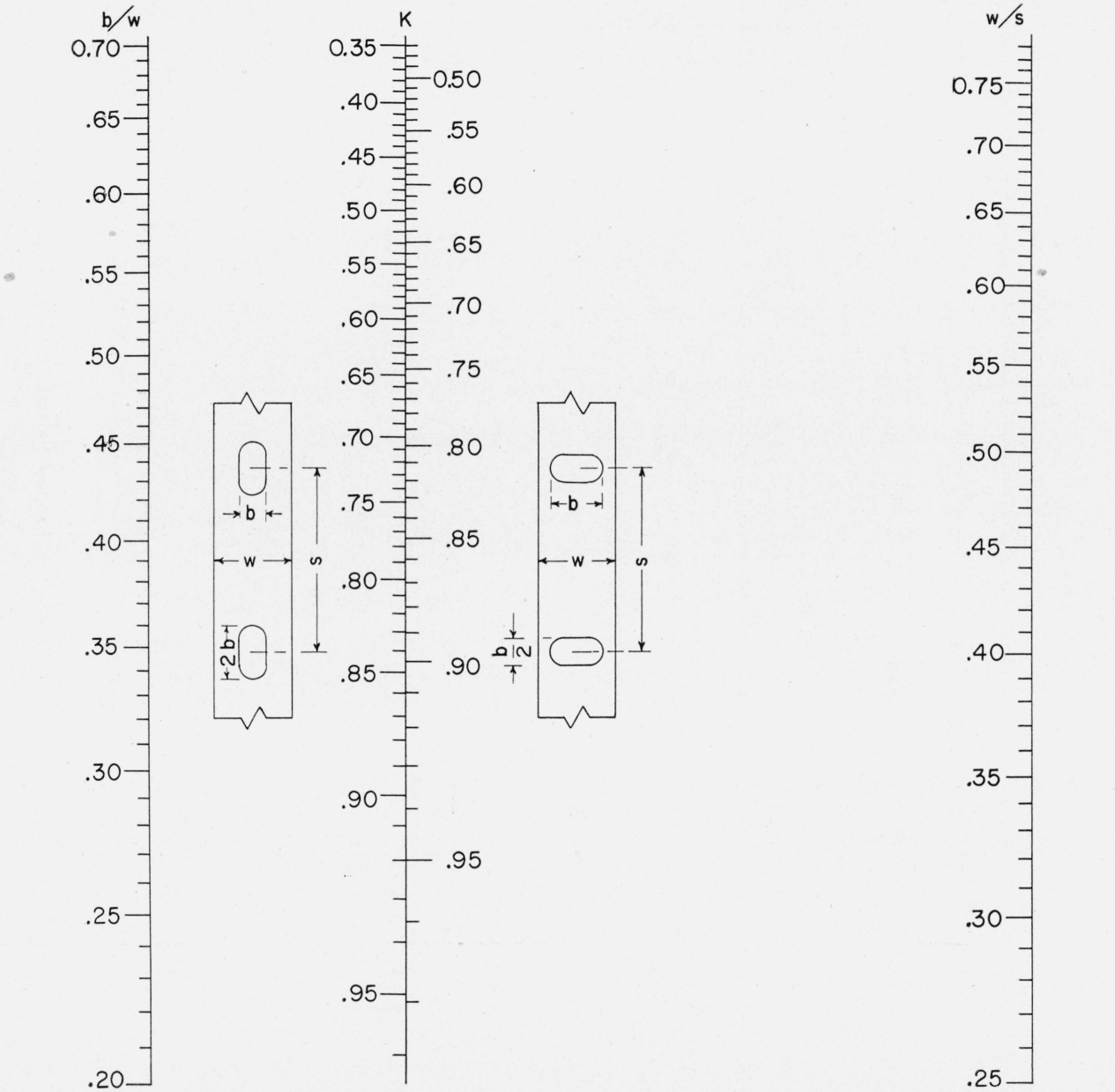


FIGURE 1. *Axial rigidity factor K of a plate of uniform thickness, having equally spaced ovaloid perforations* (eq 5).
The $K$-scale at the left is for plates in which the long axis of the perforation is parallel to the direction of the load; the $K$-scale at the right for plates in which the short axis is parallel to the load. Gross area basis.

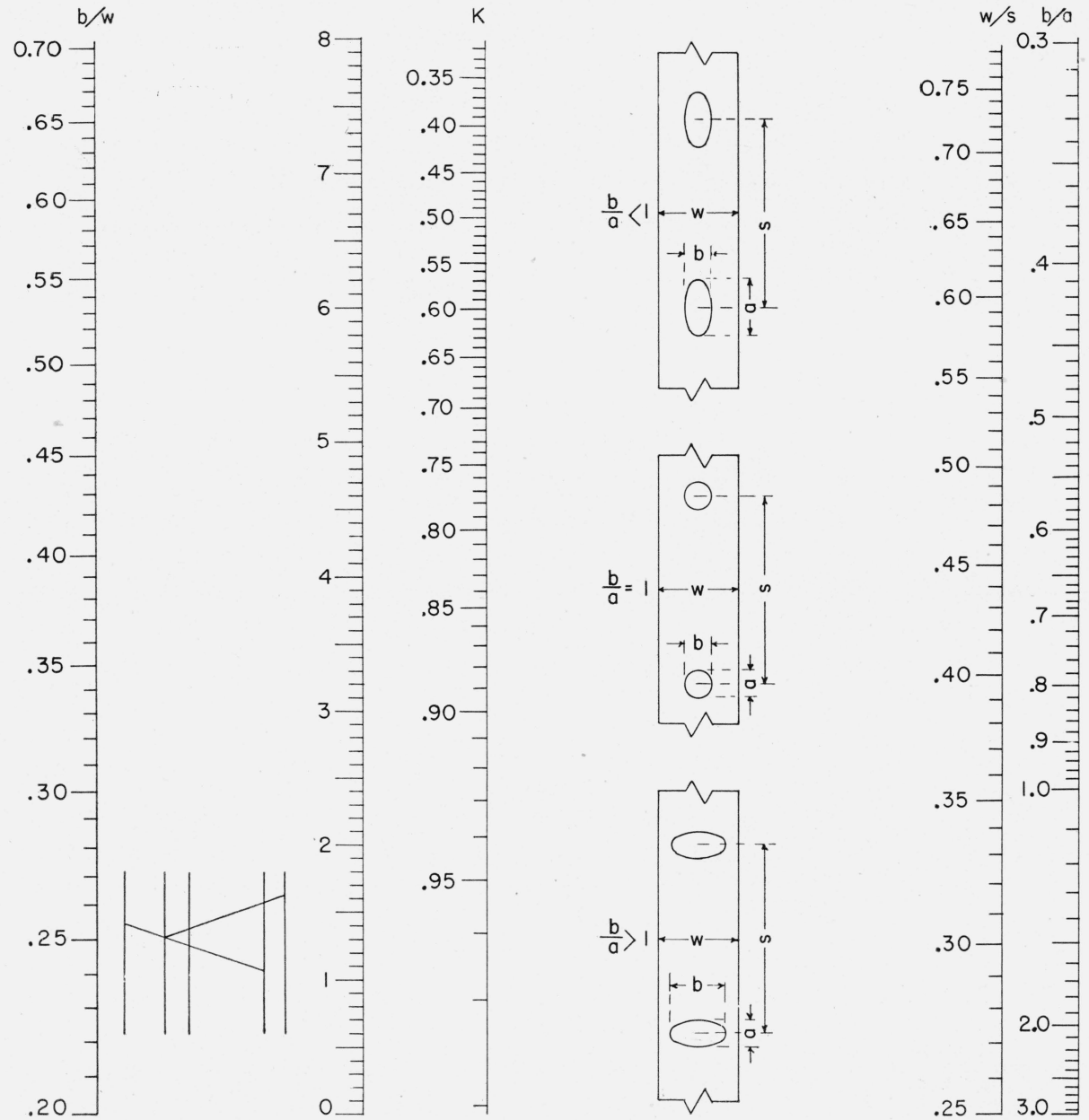


FIGURE 2. *Axial rigidity factor K of a plate of uniform thickness, having equally spaced elliptical perforations* (eq 5).
Note the key near the lower left corner. Gross area basis.

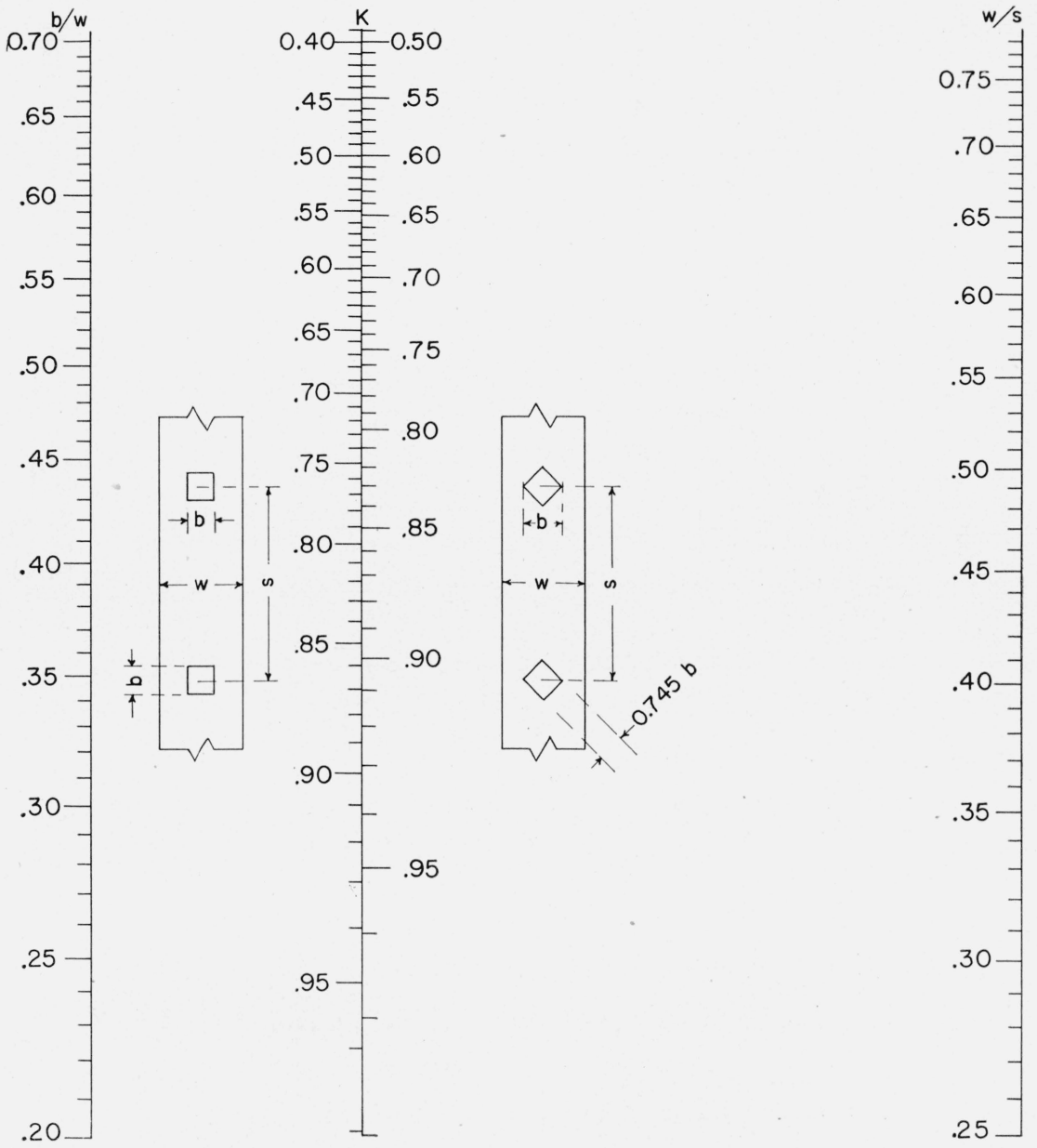


FIGURE 3. *Axial rigidity factor K of a plate of uniform thickness, having equally spaced square perforations* (eq 5).
The *K*-scale at the left is for plates in which two sides of the square are parallel to the direction of the load; the *K*-scale at the right, for plates in which diagonal of the square is parallel to the load.

TABLE 3. *Comparison of experimental and theoretical axial rigidity factors, K, for the columns and plates*

| Column designation | Number of angles | See NBS Research Paper | Axial rigidity factor, $K$, for column | | | | Axial rigidity factor, $K$, for plate | | | |
|---|---|---|---|---|---|---|---|---|---|---|
| | | | Experimental (eq 1) | | | Theoretical (eq 3) | Experimental (eq 2) | | | Theoretical (eq 3, 5) |
| **PERFORATIONS, CIRCULAR** | | | | | | | | | | |
| C1A | 2 | RP1527 | 0.853 | 0.857 | 0.857 | 0.846 | 0.63 | 0.64 | 0.64 | 0.66 |
| | 4 | do | .908 | .915 | .911 | .899 | .62 | .65 | .65 | .66 |
| C1B | 2 | do | .887 | .887 | .887 | .896 | .71 | .71 | .71 | .76 |
| | 4 | do | .928 | .928 | .925 | .933 | .71 | .72 | .70 | .76 |
| C1C | 2 | do | .912 | .912 | .912 | .922 | .78 | .77 | .77 | .81 |
| | 4 | do | .942 | .939 | 942 | .950 | .78 | .76 | .76 | .81 |
| C6 | 4 | RP1540 | .922 | .909 | ---------- | .919 | .80 | .76 | ---------- | .78 |
| **PERFORATIONS, OVALOID, LOAD PARALLEL TO LONG AXIS** | | | | | | | | | | |
| C2A | 2 | RP1474 | 0.866 | 0.874 | 0.877 | 0.874 | 0.60 | 0.62 | 0.62 | 0.67 |
| | 4 | do | .921 | .928 | .928 | .921 | .62 | .65 | .64 | .67 |
| C2B | 2 | do | .918 | .918 | .928 | .910 | .75 | .75 | .78 | .75 |
| | 4 | do | .946 | .942 | .946 | .945 | .72 | .71 | .73 | .75 |
| C2C | 2 | do | .931 | .935 | .938 | .931 | .79 | .80 | .81 | .80 |
| | 4 | do | .962 | .952 | .962 | .958 | .81 | .77 | .81 | .80 |
| C3A | 2 | RP1514 | .847 | .840 | .843 | .834 | .61 | .60 | .60 | .65 |
| | 4 | do | .908 | .905 | .908 | .891 | .64 | .62 | .64 | .65 |
| C3B | 2 | do | .867 | .867 | .874 | .876 | .67 | .67 | .68 | .72 |
| | 4 | do | .918 | .918 | .918 | .920 | .68 | .67 | .68 | .72 |
| C3C | 2 | do | .880 | .877 | .880 | .901 | .70 | .69 | .69 | .77 |
| | 4 | do | .918 | .925 | .925 | .936 | .67 | .70 | .69 | .77 |
| C4A | 2 | RP1501 | .826 | .826 | .826 | .799 | .62 | .62 | .62 | .62 |
| | 4 | do | .888 | .892 | .888 | .862 | .61 | .63 | .61 | .62 |
| C4B | 2 | do | .840 | .837 | .837 | .842 | .65 | .64 | .64 | .69 |
| | 4 | do | .895 | .888 | .892 | .893 | .64 | .62 | .63 | .69 |
| C4C | 2 | do | .864 | .860 | .857 | .870 | .70 | .69 | .69 | .74 |
| | 4 | do | .905 | .902 | .902 | .913 | .67 | .66 | .66 | .74 |
| C4E | 2 | RP1861 | .923 | .917 | .924 | .931 | .83 | .82 | .83 | .86 |
| C4F | 2 | do | .722 | .726 | .727 | .755 | .39 | .40 | .40 | .54 |
| C7 | 4 | RP1540 | .906 | .889 | ---------- | .907 | .75 | .71 | ---------- | .77 |
| **PERFORATIONS, ELLIPTICAL, LOAD PARALLEL TO MAJOR AXIS** | | | | | | | | | | |
| C4G | 2 | RP1861 | 0.838 | 0.836 | 0.836 | 0.861 | 0.64 | 0.64 | 0.64 | 0.72 |
| **PERFORATIONS, OVALOID, LOAD PARALLEL TO SHORT AXIS** | | | | | | | | | | |
| C4H | 2 | RP1861 | 0.839 | ---------- | ---------- | 0.848 | 0.65 | ---------- | ---------- | 0.70 |
| **PERFORATIONS, SQUARE, LOAD PARALLEL TO SIDE** | | | | | | | | | | |
| C4I | 2 | RP1861 | 0.828 | ---------- | ---------- | 0.833 | 0.63 | ---------- | ---------- | 0.68 |
| **PERFORATIONS, SQUARE, LOAD PARALLEL TO DIAGONAL** | | | | | | | | | | |
| C4J | 2 | RP1861 | 0.855 | ---------- | ---------- | 0.880 | 0.69 | ---------- | ---------- | 0.75 |

The values of the experimental and the theoretical axial rigidity factors for the columns and for the plates are given in table 3. The experimental values have been plotted against the theoretical values in figure 4 for the columns and in figure 5 for the plates. In figures 4 and 5 the shape of the perforation is indicated by the shape of the plotted symbol, and the direction of the load was parallel to the ordinates.

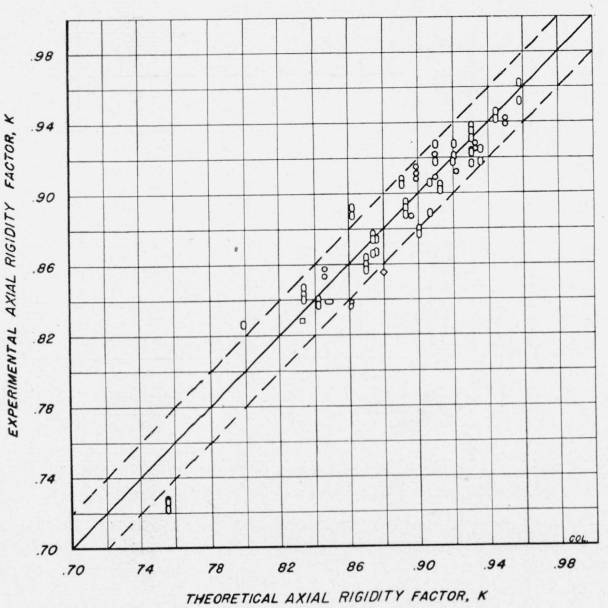


FIGURE 4. *Relation between experimental and theoretical axial rigidity factors for the columns.*

Based on gross area.

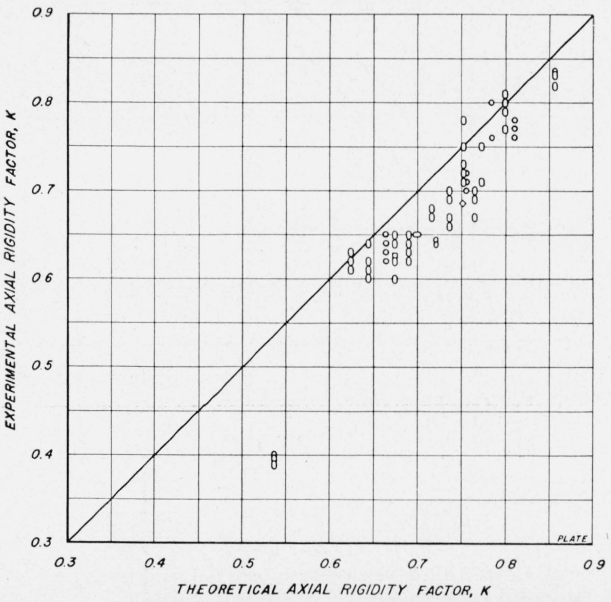


FIGURE 5. *Relation between experimental and theoretical axial rigidity factors for the perforated plates.*

Based on gross area

The experimental and theoretical values of $K$ for the columns, figure 4 and table 3, differed by not more than $\pm 0.02$, except for a few scattered values. Only one set of data is available for $K$ less than 0.76.

When the perforated plates are considered, as shown in figure 5 and table 3, the agreement between experimental and theoretical values is also good, although not as good as for the complete columns. The general tendency is for the experimental values to be less than the theoretical. The difference is considerable for theoretical values of $K$ for the plate less than about 0.55. It is probable that perforations relatively as large as these (columns C4F, reference [4]) will seldom be used in practice. The limitations of eq 3 have been discussed by Greenspan in reference [5, p. 319]. The results of these tests then show that the axial rigidity factor of columns and of perforated plates can be closely approximated by calculations according to eq 3 or 5.

## III. Stresses on the Edge of the Perforation

Many theoretical studies of the influence of a perforation on the stresses in a plate loaded, say in the direction of its length, are based on the assumption that the plate width is large in comparison to the perforation width. Stresses $\sigma$ at a point near the perforation are then compared with the uniform stress, $S$, at a large distance from the hole, generally by evaluating the ratio $\sigma/S$. In other similar studies but for a plate having a finite width and gross area $A_g$ subjected to a load $P$, it has been found [6, 8] that instead of using the average stress based on gross area, $P/A_g$, for comparison with values derived from consideration of an infinite plate, the correction factor $C(n)$ of eq 4 should be used for the stress ratios, as $\sigma C(n)/(P/A_g)$. The value of $(Cn)$ is unity for an infinite plate and is always less than one for a plate or column of finite cross-sectional area.

If experimental stress ratios determined for a column having a finite cross-sectional area are to be compared with theoretical values derived for an infinite plate, the observed stress ratio $\sigma_{uv}/(P/A_g)$ should be reduced in value by multiplying it by the $C(n)$ correction factor for the column, where $\sigma_u$ is the maximum principal stress and $\sigma_v$ the minimum principal stress.

Conversely, if the theoretical stress ratios, derived for an infinite plate, are to be compared to experimental values for a column of finite cross-sectional area, the former values should be increased by dividing them by the $C(n)$ correction factor to obtain theoretical value for a column of finite cross-sectional area, defined by $C(n)$.

The distributions of stresses on the edge of the middle perforation, averaged for all columns having perforations of the same shape and loaded in the same direction, are shown by the solid lines in figures 6, 7, 8, 9, 10, and 11. These values are based on gross area. The rectified lengths of one quadrant of the perforation boundaries were reduced to a standard length $AC$. Before averaging, the experimental stress ratio values were multiplied by the $C(n)$ value for the column, as given in table 4.

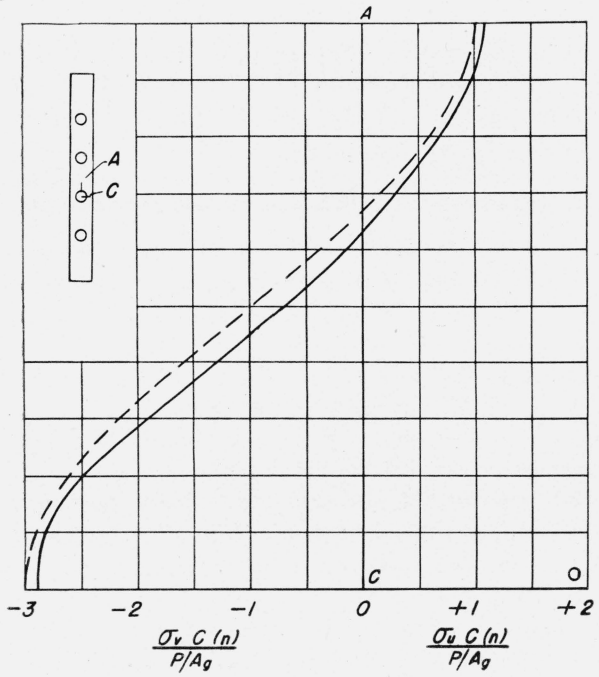


FIGURE 6. *Circular perforations; distribution of stress on the edge of the perforation.*

The solid line is the average of the experimental values multiplied by $C(n)$ for 19 columns. The dashed line represents the theoretical distribution. Based on gross area.

The dashed lines of figures 6 to 11 represent the theoretical stress distribution at the boundary of a single perforation in an infinite plate, according to the formulas of reference [7].

As the experimental stress ratios have been multiplied by the $C(n)$ correction factor, they are in effect representative of stress ratios in an

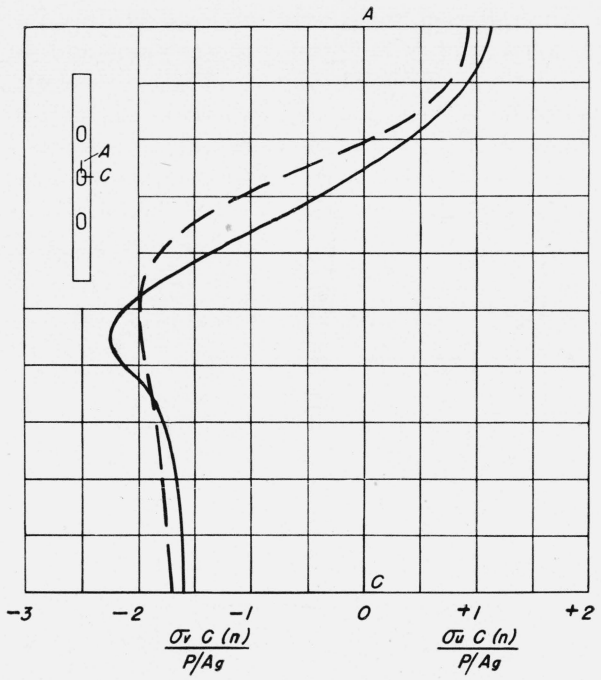


FIGURE 7. *Ovaloid perforations; load parallel to long axis; distribution of stress on the edge of the perforation.*

The solid line is the average of the experimental values multiplied by $C(n)$ for 61 columns. The dashed line represents the theoretical distribution. Based on gross area.

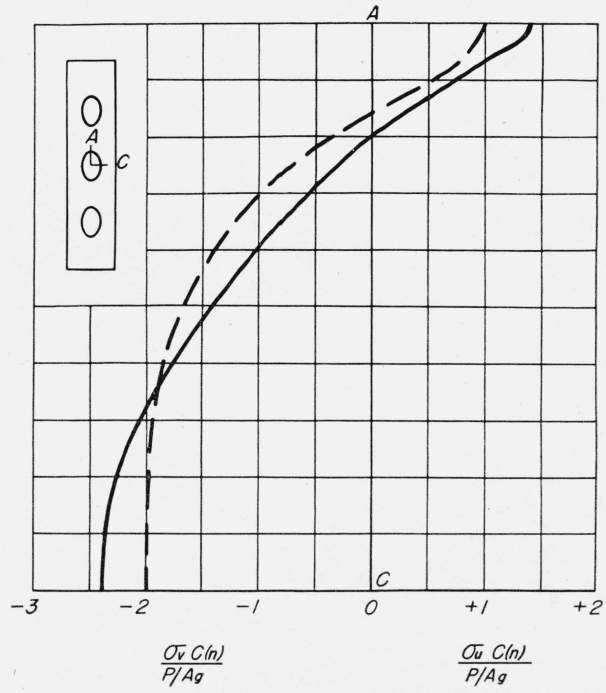


FIGURE 8 *Elliptical perforations; load parallel to major axis; distribution of stress on the edge of the perforation.*

The solid line shows the experimental values multiplied by $C(n)$ for column C4G–2. The dashed line represents the theoretical distribution. Based on gross area.

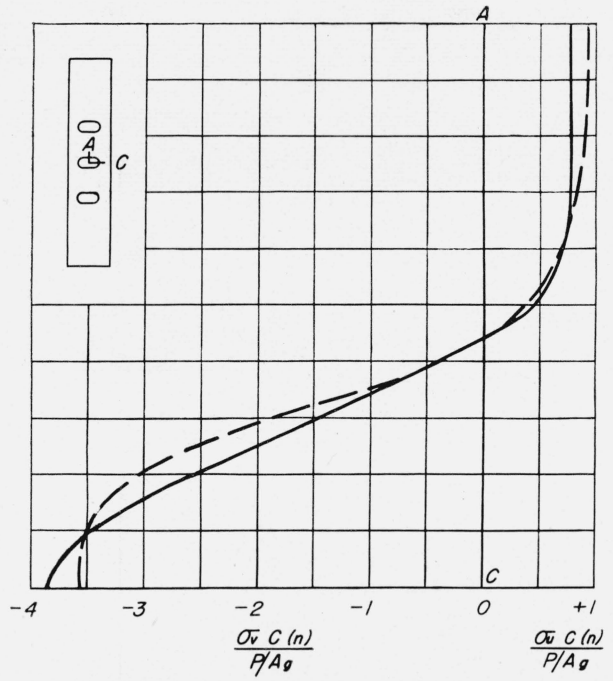


FIGURE 9. *Ovaloid perforations; load parallel to short axis; distribution of stress on the edge of the perforation.*

The solid line shows the experimental values multiplied by $C(n)$ for column C4H. The dashed line represents the theoretical distribution. Based on gross area.

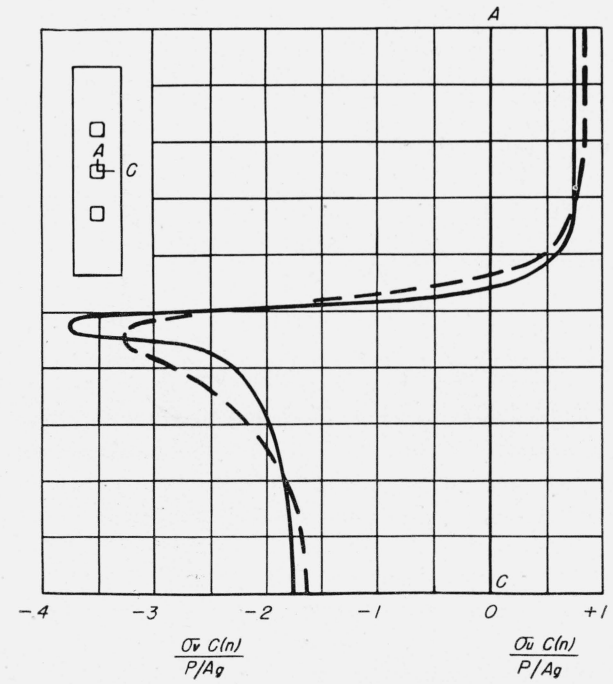


FIGURE 10. *Square perforations; load parallel to two sides; distribution of stress on the edge of the perforation.*

The solid line shows the experimental values multiplied by $C(n)$ for column C4I. The dashed line represents the theoretical distribution. Based on gross area.

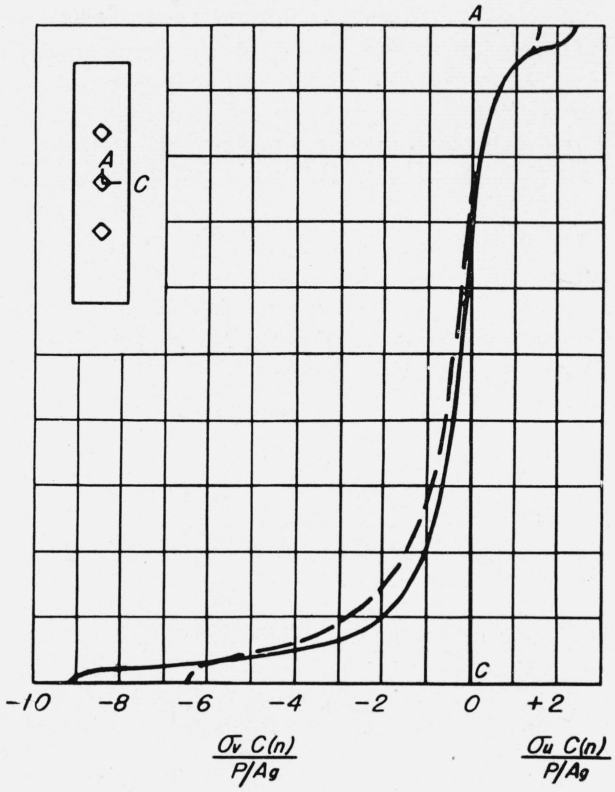


FIGURE 11. *Square perforations, load parallel to diagonal; distribution of stress on the edge of the perforation.*

The solid line shows the experimental values multiplied by $C(n)$ for column C4J. The dashed line represents the theoretical distribution. Based on gross area.

infinite plate and may be compared with the theoretical values, the derivation of which was based on the conditions in an infinite plate.

The agreement between the theoretical and experimental stress distributions on the edge of the perforation is good in all cases.

It should be noted that the theoretical stress distribution was derived by considering a plate having a single hole, and the observed stress ratios were obtained for plates having a series of equally spaced similar perforations.

It was decided to tabulate the values of the maximum stress for the perforated cover plates since they are of basic importance for structural design. The maximum stress is expressed by a "maximum stress ratio", maximum stress/$(P/A_g)$. Values of maximum stress ratio are given in references [2, 3, 4] and in table 4 of this paper. The values based on gross area may be compared with the theoretical maximum stress ratios to be evaluated from the equations given in reference

TABLE 4. *Maximum stress concentration in the boundary of the perforation*

| Column designation | Number of angles | $C(n)$ | Ratio: $\frac{\text{Maximum stress}}{P/Ag}$, based on gross area | | | | | Ratio: $\frac{\text{Maximum stress}}{P/Ag}$ based on net area of experimentally tested column | | |
|---|---|---|---|---|---|---|---|---|---|---|
| | | | Theoretical | | Experimentally tested column | | | | | |
| | | | Infinite plate | Tested column | | | | | | |
| PERFORATIONS—CIRCLES | | | | | | | | | | |
| C1A, C1B, C1C | 4 | 0.994 | 3.00 | 3.02 | 2.50 | 2.91 | 3.06 | 2.22 | 2.59 | 2.72 |
| Do | 2 | .984 | 3.00 | 3.05 | 2.77 | 3.24 | 3.43 | 2.28 | 2.67 | 2.82 |
| C6 | 4 | .992 | 3.00 | 3.02 | 2.58 | | | 2.26 | | |
| PERFORATIONS—OVALOIDS, LOAD PARALLEL TO LONG AXIS | | | | | | | | | | |
| C2A, C2B, C2C | 4 | 0.996 | 1.96 | 1.97 | 2.03 | 2.20 | 2.20 | 1.85 | 2.01 | 2.01 |
| Do | 2 | .989 | 1.96 | 1.98 | 2.15 | 2.43 | 2.52 | 1.83 | 2.07 | 2.15 |
| C3A, C3B, C3C | 4 | .994 | 1.96 | 1.97 | 1.97 | 2.28 | 2.39 | 1.75 | 2.03 | 2.13 |
| Do | 2 | .984 | 1.96 | 1.99 | 2.16 | 2.37 | 2.55 | 1.78 | 1.95 | 2.10 |
| C4A, C4B, C4C | 4 | .991 | 1.96 | 1.98 | 1.98 | 2.27 | 2.43 | 1.72 | 1.97 | 2.11 |
| Do | 2 | .979 | 1.96 | 2.00 | 2.24 | 2.63 | 2.48 | 1.78 | 2.09 | 1.97 |
| C4E | 2 | .993 | 1.96 | 1.97 | 2.28 | | | 2.01 | | |
| C4F | 2 | .957 | 1.96 | 2.05 | 2.39 | | | 1.69 | | |
| C7 | 4 | .992 | 1.96 | 1.98 | 2.18 | | | 1.91 | | |
| PERFORATIONS—OVALOIDS, LOAD PARALLEL TO SHORT AXIS | | | | | | | | | | |
| C4H | 2 | 0.979 | 3.57 | 3.65 | 3.94 | | | 3.12 | | |
| PERFORATIONS—ELLIPSES, LOAD PARALLEL TO MAJOR AXIS | | | | | | | | | | |
| C4G | 2 | 0.979 | 2.00 | 2.04 | 2.43 | | | 1.93 | | |
| PERFORATIONS—SQUARES, LOAD PARALLEL TO SIDE | | | | | | | | | | |
| C4I | 2 | 0.979 | 3.28 | 3.35 | 3.82 | | | 3.02 | | |
| PERFORATIONS—SQUARES, LOAD PARALLEL TO DIAGONAL | | | | | | | | | | |
| C4J | 2 | 0.978 | 6.45 | 6.60 | 9.70 | | | 7.41 | | |

[7]. The theoretical maximum stress ratios are given for the columns in table 4, for both an infinite plate and for the actual column.

The three experimental maximum stress ratios given in the same line of table 4 are for columns having perforations of the same size but for increasing perforation spacings, as given in table 1. There seems to be a tendency in many cases for the experimental maximum stress ratio to increase as the perforation spacing increases.

The experimental values based on gross area are in many cases greater than the theoretical maximum stress ratios for the tested columns.

It is also interesting to compare the theoretical maximum stress ratios with the experimental values that are based on net area, even though such a comparison runs counter to some of the assumptions involved in the theoretical derivations. The values are also given in table 4. Very few of the experimental maximum stress ratios based on net area are greater than the theoretical values for the tested columns. The spread between the gross and net areas in nearly all commercial structural columns would be less than for these columns that have been tested. It would seem then that the theoretical maximum

stress ratios, determined as described above, can be safely used for designing perforated plate columns.

## IV. Tests to Failure to Determine Maximum Compressive Loads

The steel columns subjected to compressive test to destruction consisted of a plate and two angles except for columns C6 and C7 [3], which had four angles. Unfortunately the C6 and C7 column series did not contain any columns with solid plates for comparison with the strengths of those perforated plate columns.

The other columns had cross-sectional shapes as shown in figure 12. The distance $y_p$ from the the back of the plate to the center of area of the section, in the perforated portion of a column is always greater than the similar distance, $y_s$, for the solid portion of a perforated plate column. There is therefore a local eccentricity, $y_p - y_s$, tending to induce increased compression in the plate and to make the column fail by bending away from the plate side during a compressive load test. Tests of columns of this shape would thus be expected to give lower compressive strength values than would tests of columns of the same quality in which the perforated plates were not eccentrically loaded, as would be the case for four angle columns.

Of the four columns having two angles and a solid plate, two failed by primary buckling, bending toward the plate side as would be expected from the double modulus column theory. The other two columns began to deflect toward the plate side but finally failed by secondary buckling of the plate and deflected away from the plate side.

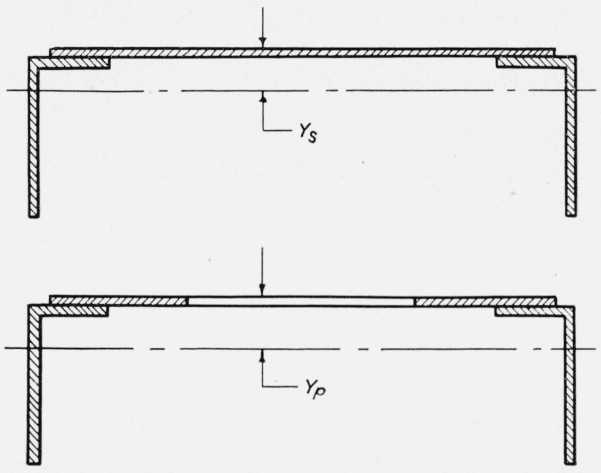


FIGURE 12. *Cross sections of columns having two angles.*

Top, the section representing a column having a solid plate or a section through the solid portion of a perforated plate column. Bottom, a section through the perforation. Eccentricity $= y_p - y_s$.

Of the 24 columns having two angles and a perforated plate, 22 failed by bending away from the plate side as would be expected from the consideration that, in the neighborhood of a perforation, the gravity axis of the columns is displaced away from the plate side. The other two columns showed practically no deflection until the maximum load was very nearly reached and then failed by bending toward the plate side.

The four columns, each having four angles and a perforated plate, all failed by buckling of the plates near one of the perforations.

The final failure of all of the columns was accompanied by local buckling of the outstanding legs of the angles, and by buckling of the plate near a perforation for the perforated plate columns as well as the general bending of the columns as a whole.

Figure 13 shows the perforated plate column C4J in the testing machine for the maximum load test.

The slenderness ratio for the solid plate columns was 70 for column C2, 71 for columns C1 and C3, and 72.5 for columns C4.

The effective area factor $C$ of a perforated plate is a measure of the effectiveness of the plate with regard to compressive strength. It can be calculated, as shown on p. 685 of reference [1] by the formula

$$C = \frac{P_{\max}}{A_p \sigma_{\max}} - \frac{A_a}{A_P} \tag{6}$$

where $P_{\max}$ is the total compressive load at failure for the perforated plate column, $\sigma_{\max}$ is the average stress obtained by dividing the maximum compressive load on a similar solid plate column by the gross cross-sectional area, $A_a$ the cross-sectional area of the angles and $A_p$ the cross-sectional area of the plate. $C$ may be taken on a gross- or on a net-area basis, depending on which value of $A_p$ is used.

When based on net area, the value of $C$ would be unity if the average compressive stress at failure for the perforated plate column was equal to that of a similar column having a solid plate.

Values of the effective area factor, $C$, for the two-angle columns are given in table 5.

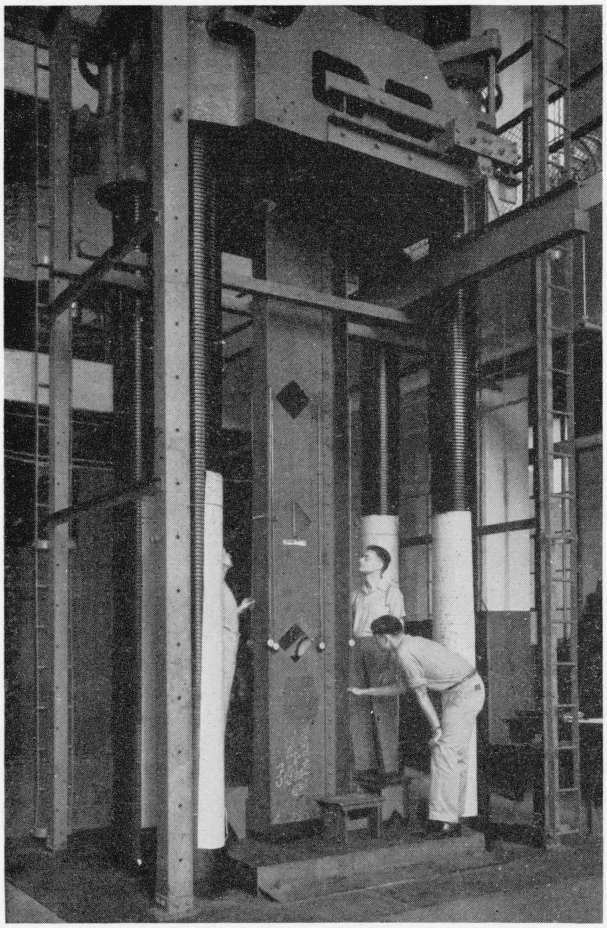

FIGURE 13. *Column C4J in the testing machine during the maximum compressive load test.*

The effective area factor $C$ based on net area was for all but three columns greater than unity. For these C2 columns, the compressive stress at failure, based on net area, was 32.7 kips/in.$^2$ for C2A; 32.3 kips/in.$^2$ for C2B; and 33.3 kips/in.$^2$ for C2C. The compressive stress at failure for the similar column C2D having a solid plate was 33.8 kips/in$^2$. The effective area factor $C$ for columns of the size tested is evidently very sensitive to relatively small differences of compressive stress at failure.

From a consideration of these effects and of the local eccentricities present in perforated plate columns having but two angles, it seems that the net area of perforated steel plates may safely be used for design purposes. The values of table 5 show this is true for perforations of all of the shapes tested, even those having relatively great values of the maximum stress ratios.

TABLE 5. *Effective area factor, C, with respect to compressive strength for the columns*

[Each column had a perforated plate and two angles]

| Column designation | Effective area factor, $C$ | |
|---|---|---|
| | Based on gross area | Based on net area |
| PERFORATIONS—CIRCLES | | |
| C1A | 0.68 | 1.22 |
| C1B | .68 | 1.22 |
| C1C | .74 | 1.35 |
| PERFORATIONS—OVALOIDS, LOAD PARALLEL TO LONG AXIS | | |
| C2A | 0.47 | 0.85 |
| C2B | .44 | .79 |
| C2C | .52 | .93 |
| C3A | .59 | 1.06 |
| C3B | .57 | 1.03 |
| C3C | .64 | 1.16 |
| C4A | .62 | 1.12 |
| C4B | .65 | 1.18 |
| C4C | .71 | 1.28 |
| C4E–1 | .93 | 1.25 |
| C4E–2 | .83 | 1.13 |
| C4E–3 | .91 | 1.23 |
| C4F–1 | .48 | 1.35 |
| C4F–2 | .52 | 1.45 |
| C4F–3 | .46 | 1.31 |
| PERFORATIONS—ELLIPTICAL, LOAD PARALLEL TO MAJOR AXIS | | |
| C4G–1 | 0.76 | 1.38 |
| C4G–2 | .72 | 1.31 |
| C4G–3 | .75 | 1.36 |
| PERFORATIONS—OVALOID, LOAD PARALLEL TO SHORT AXIS | | |
| C4H | 0.64 | 1.18 |
| PERFORATIONS—SQUARE, LOAD PARALLEL TO SIDE | | |
| C4I | 0.73 | 1.33 |
| PERFORATIONS—SQUARE, LOAD PARALLEL TO DIAGONAL | | |
| C4J | 0.75 | 1.39 |

## V. Summary and Conclusions

Tests in the elastic range have been made on 88 steel columns with perforated plates and on 17 steel columns with solid plates. Maximum compressive load tests have been made on 28 columns with perforated plates and on 4 with solid plates.

Theories have been derived dealing with the

axial rigidity of perforated plate columns and with the stress distribution in the neighborhood of a perforation.

Comparisons between the test results and the theoretical values lead to the conclusions that the axial rigidity is correctly defined by the theoretical eq 3 of this paper; and that the distribution of stress on the boundary of a perforation is adequately expressed by the equations of reference [7].

The results of the maximum compressive-load tests show that the net area of perforated plate columns may safely be used for estimating the strength of columns with perforated cover plates.

---

The tests of perforated cover plates for steel columns have been made in cooperation with the American Institute of Steel Construction, which furnished the specimens. The program was prepared by the National Bureau of Standards and by the Institute's Committee on Technical Research, which at the start of the program consisted of Comfort A. Adams, the late Otis E. Hovey, H. D. Hussey, Jonathan Jones, the late J. R. Lambert, the late L. S. Moisseiff, Walter Weiskopf, and F. H. Frankland, chairman. The committee was assisted by Shortridge Hardesty, Frank M. Masters, and Henry C. Tammen. The work was done in the Engineering Mechanics Section of the National Bureau of Standards.

The Institute has expressed no disapproval because the final tests were delayed for 4 years because of the Second World War. This forbearance has been much appreciated by the members of the staff to whom this work was assigned.

## VI. References

[1] Ambrose H. Stang and Martin Greenspan, J. Research NBS **28,** 669 (1942) RP1473.

[2] Ambrose H. Stang and Martin Greenspan, J. Research NBS **28,** 687 (1942) RP1474; **29,** 279 (1942) RP1501; **30,** 15 (1943) RP1514; **30,** 177 (1943) RP1527.

[3] Ambrose H. Stang and Martin Greenspan, J. Research NBS **30,** 411 (1943) RP1540.

[4] Ambrose H. Stang and Bernard S. Jaffe, J. Research NBS **40,** 121 (1948) RP1861.

[5] Martin Greenspan, J. Research NBS **31,** 305 (1943) RP1568.

[6] Martin Greenspan, J. Research NBS **37,** 157 (1946) RP1737.

[7] Martin Greenspan, Quart. Applied Math. **2** 60 (1944).

[8] E. G. Coker and L. N. G. Filon, A treatise on photoelasticity, p. 545 (Cambridge Univ. Press, Cambridge, Eng., 1931).

WASHINGTON, November 28, 1947.